IEEE Photonics Journal
An IEEE Photonics Society Publication

Wavelength-Switchable and Wavelength-Tunable All-Normal-Dispersion Mode-Locked Yb-Doped Fiber Laser Based on Single-Walled Carbon Nanotube Wall Paper Absorber

Volume 4, Number 1, February 2012

Xiao-Hui Li
Yong-Gang Wang
Yi-Shan Wang
Xiao-Hong Hu
Wei Zhao
Xiang-Lian Liu
Jia Yu
Cun-Xiao Gao
Wei Zhang
Zhi Yang
Cheng Li
De-Yuan Shen

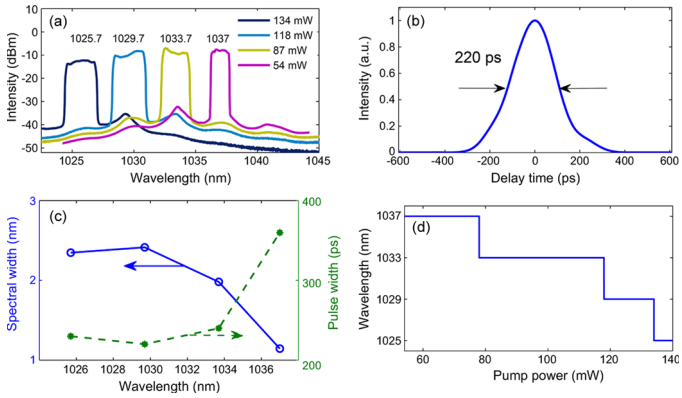

DOI: 10.1109/JPHOT.2012.2183862
1943-0655/$31.00 ©2012 IEEE

Wavelength-Switchable and Wavelength-Tunable All-Normal-Dispersion Mode-Locked Yb-Doped Fiber Laser Based on Single-Walled Carbon Nanotube Wall Paper Absorber

Xiao-Hui Li,[1,2] Yong-Gang Wang,[3] Yi-Shan Wang,[1] Xiao-Hong Hu,[1] Wei Zhao,[1] Xiang-Lian Liu,[1,2] Jia Yu,[1] Cun-Xiao Gao,[1] Wei Zhang,[1] Zhi Yang,[1] Cheng Li,[1] and De-Yuan Shen[1]

[1]State Key Laboratory of Transient Optics and Photonics, Xi'an Institute of Optics and Precision Mechanics, Chinese Academy of Sciences, Xi'an 710119, China
[2]School of Science, Xi'an Jiaotong University, Xi'an 710049, China
[3]Department of Applied Physics, The Hong Kong Polytechnic University, Hong Kong

DOI: 10.1109/JPHOT.2012.2183862

Manuscript received December 28, 2011; accepted January 6, 2012. Date of publication January 11, 2012; date of current version January 31, 2012. This was supported by The CAS Special Grant for Postgraduate Research, Innovation and Practice and by the National Natural Science Foundation of China under Grant 61107034. Corresponding author: Y.-S. Wang (e-mail: yshwang@opt.ac.cn).

Abstract: We demonstrate a compact wavelength-tunable and -switchable mode-locked Yb-doped fiber (YDF) laser based on single-walled carbon nanotube (SWCNT) wall paper absorber. Two mechanisms coexist in the fiber cavity. The switchable mode-locked state can be obtained between two wavelengths depending on the fiber-loop-induced cavity birefringence. Because of the intensity-dependent transmission distribution, the proposed fiber laser can be operated in the tunable wavelength mode-locked state from 1025 to 1037 nm. The spectral bandwidth varied from 1.1 to 2.4 nm depending on the operating wavelength and the pump power with pulse duration of hundreds of picoseconds. The average wavelength spacing is 3.6 nm, which can be changed, corresponding to the birefringence of the fiber cavity. Moreover, stable wavelength-tunable mode locking is obtained at room temperature.

Index Terms: Fiber lasers, mode-locked lasers, tunable lasers, carbon nanotubes and confined systems.

1. Introduction

Wavelength-tunable and wavelength-switchable mode-locked fiber lasers have potential applications in wavelength-division-multiplexed (WDM) communication systems, fiber sensing, optical signal processing, spectroscopy, and biomedical researches and are being studied intensively. Various methods have been utilized to achieve tunable and switchable wavelength mode-locked fiber lasers [1]–[12]. Nonlinear polarization rotation (NPR) techniques have been utilized to achieve tunable multiwavelength operation in fiber ring cavities [3], [4]. Optical filters utilized to achieve tunable mode locking in a fiber laser have been demonstrated [7]. It has also been reported that tunable wavelength mode-locked fiber lasers can be realized based on a nonlinear optical loop mirror (NOLM) or on polarization-maintaining fiber (PMF) [5], [8], [10]. In addition, wavelength-tunable mode-locked lasers can be obtained with the active mode-locked technique, which is generally

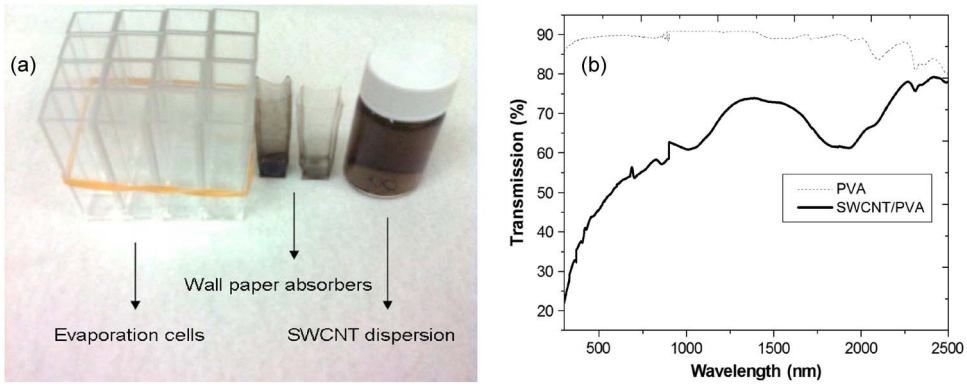

Fig. 1. (a) Left: Polystyrene cell for the growth of absorber. Right: SWCNT/PVA dispersion. The wall paper absorber with different density of SWCNT is in the middle. (b) Linear transmission curves of PVA wall paper and SWCNT/PVA wall paper absorber.

realized by inserting an electrooptic modulator in the laser cavity. However, the actively mode-locked lasers are bulky, expensive and have the drawbacks of weak peak power because of the modulator in the cavity.

Recently, single-walled carbon nanotubes (SWCNTs) with uniformly distributed diameters and chiralities as well as other novel saturable absorbers have broadband saturable absorption and can be used to achieve mode locking in a wide tunable wavelength range [13]–[17]. Usually, the tunable mode locking can be achieved together with other additional components (such as tunable filter, PMF, attenuator or fiber gratings), which destroy the simple and compact structure of the fiber laser. Is it possible to use other mechanism to obtain the wavelength-switchable and wavelength-tunable mode locking while keeping the compact structure of the fiber cavity?

In this paper, the switchable and tunable wavelength mode-locked Yb-doped fiber (YDF) laser is demonstrated based on SWCNT wall paper absorber. Two mechanisms are responsible for the realization of switchable and tunable mode locking. One is the fiber cavity birefringence; the other is the intensity-dependent transmission distribution. Because of the cavity birefringence, a switchable wavelength mode-locked fiber laser is obtained. A tunable wavelength can be achieved by varying the pump power. With the two mechanisms in the cavity, the proposed fiber laser can be mode-locked over a wavelength range from 1025 to 1037 nm with a spacing of about 3.6 nm. Moreover, stable wavelength-tunable mode locking is thus obtained at room temperature.

2. Experimental Setup

The SWCNTs used in this experiment were grown by electric arc discharge technique. The mean diameter of the SWCNTs is about 1.5 nm. First, several milligrams of SWCNT powder were poured into 10 ml 0.1% sodium dodecyl sulfate (SDS) aqueous solution. Here, SDS was used as a surfactant. In order to obtain SWCNT aqueous dispersion with high absorption, SWCNT aqueous solution was ultrasonically agitated for 10 h. After the ultrasonic process, the dispersed solution of SWCNT was centrifuged to induce sedimentation of large SWCNT bundles. After decanting the upper portion of the centrifuged solution, some PVA powder was poured into the solution and dissolved at 90 °C with ultrasonic agitation for 3 h. Then, the SWCNT/PVA dispersion was diluted and poured into a polystyrene cell, as shown in Fig. 1(a). Finally, we put these cells in an oven for evaporation. The temperature of the oven was kept at 40 °C or 45 °C. It took about one or two days for complete evaporation. When the evaporation was finished, the wall and the bottom of the cell were coated with a thin plastic film. The PVA aqueous solution has strong viscosity to the polystyrene cell so that it adheres to the wall of the cell. When the cell was dry, the PVA film lost the viscosity to the cell. Therefore, we can strip the PVA film cell off the polystyrene cell easily with tweezers. The SWCNTs were carried by PVA to the surface of the wall and the bottom of the polystyrene cell during the evaporation process. The SWCNT/PVA film on the wall of the cell had

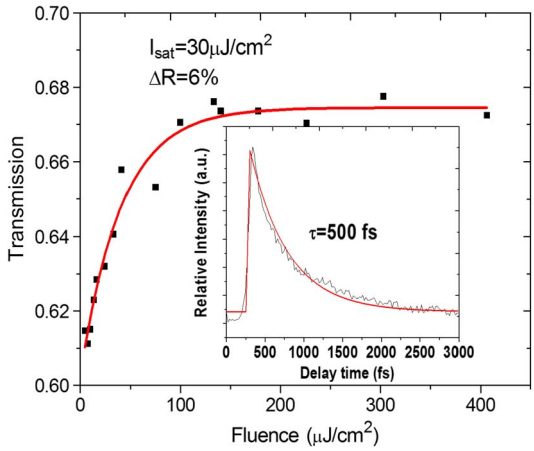

Fig. 2. Transmission of wall paper absorber with the increase of pump fluence; inset is the recovery time of the absorber.

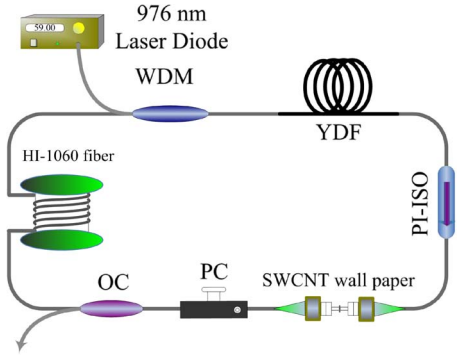

Fig. 3. Schematic of the mode-locked fiber laser based on SWCNT wall paper absorber.

higher quality than that on the bottom; therefore, we can use the former as absorber for mode locking, and hereafter, we call it the "SWCNT wall paper absorber" [18]. The procedure to fabricate the wall paper absorber is very simple. In practice, we cut off the wall paper absorber cell into many pieces for use in mode locking.

An UV–Visible–NIR spectrophotometer was employed to measure the linear optical transmission of the PVA wall paper and SWCNT/PVA wall paper absorber, as shown in Fig. 1(b). (The PVA wall paper is fabricated by PVA solution and not the SWCNT/PVA composite dispersion.)

Fig. 2 shows the transmission of the wall paper absorber with the increase of pump fluence measured in a Spectra-Physics ultrafast laser system. We measured the modulation depth of the SWCNT absorber at 1060 nm. The modulation depth of the absorber is about 6%, and the saturable pump fluence is about 30 μJ/cm^2. The inset in Fig. 2 shows the ultrafast transient absorption trace. It reveals an instantaneous rise followed by an exponential decay with a time constant of 500 fs. The result shows that as-fabricated SWCNT absorber has a very short recovery time, which is sufficient for the ultrafast laser.

The center wavelength of emission peak for the YDF is about 1030 nm. As a result, through utilizing the emission peak and the SWCNT wall paper absorber, mode locking around 1030 nm was obtained. Fig. 3 shows the schematic diagram of the proposed fiber lasers based on the SWCNT wall paper absorber in the cavity. A 0.3-m-long YDF with absorption coefficient of 1000 dB/m at 976 nm is used as the gain medium. In order to get mode locking solely with the SWCNT wall paper absorber and force the laser to propagate unidirectionally in the cavity, a

polarization-independent isolator (PI-ISO) is used in the cavity. A polarization controller (PC) is mounted on the passive fiber to achieve different polarization orientation states in the cavity. A 10 : 90 optical coupler (OC) is used to output the signal. The other fiber in the cavity together with the pigtail of the passive components is HI-1060 fiber, and the total cavity length is 21.46 m. The dispersion of YDF is -38 ps/nm/km at 1030 nm, and the HI-1060 fiber is about -43 ps/nm/km at 1030 nm. As a result, the total dispersion of the cavity is about 0.549 ps^2. The fabricated SWCNT wall paper absorber is inserted in the cavity through transferring a piece of free standing wall paper, which is cut into 1 $\times$ 1 mm pieces, onto the end facet of a fiber pigtail via the Van der Walls force. Since the fibers in the cavity all exhibit normal dispersion, switchable and tunable dissipative solitons can be obtained. The proposed fiber laser is pumped by a 976-nm laser diode (LD).

We intentionally introduced strong cavity birefringence into the laser cavity through over bending the HI-1060 fibers into a loop on a spool that the birefringence induced filtering effect of the cavity becomes ignorable no longer. As a result, by changing the orientation of PC in the cavity, the effective gain peak of the laser can be shifted, which eventually leads to wavelength-switchable and wavelength-tunable mode-locked states. On the other hand, thanks to the wide broadband saturable absorption of the SWCNT wall paper, we can change the pump power to provide different intracavity loss-and-gain distributions, which results in the changes of the inversion condition of the YDF. The varied loss-and-gain distribution, together with the birefringence induced filtering effect, can make the tunable-center wavelength mode locking possible.

The spectra are monitored by an optical spectra analyzer (OSA, Yokogawa AQ-6370), and mode-locked pulse trains are detected with a 6-GHz digital storage oscilloscope (DSO), together with an 11-GHz photodetector (PD).

3. Experimental Results and Discussions

Switchable wavelength mode locking can be realized by varying the polarization orientation of the PC. For one polarization states, continuous wavelength (CW) emission at a center wavelength of 1037 nm can be obtained when the pump power is above 35 mW. Some periodical spectral intensity modulations appear on the spectrum, which means that it is possible to achieve mode locking at these wavelength regions. Self-starting mode locking at the center wavelength of 1037 nm can be achieved when the pump power is above 54 mW. By carefully changing the orientations of the PC, the spectral peak of 1034 nm becomes high, and the mode locking can be shifted at this wavelength. When the PC is tuned back to the former orientation state, the mode locking at 1037 nm can be obtained again. As a result, the switchable mode locking between 1033 nm and 1037 nm is realized. Dissipative solitons with steep spectral edges are always generated in the all-normal-dispersion regime [19], [20]. Fig. 4(a) shows the spectra for a pump power of 70 mW in two polarization orientation states. The spectral widths are 2.11 nm at 1033.53 nm and 1.82 nm at 1036.89 nm. The corresponding pulse durations are 237 ps (at 1033 nm) and 300 ps (at 1037 nm), as shown in Fig. 4(b). The time-bandwidth products are 140.44 and 152.35, respectively, indicating that the pulses have large chirps in the cavity. Fig. 4(c) shows the oscilloscope trace at 1036.89 nm, and the corresponding radio frequency (RF) spectrum is shown in Fig. 2(d) with a span range of 250 MHz. The inset of Fig. 4(d) corresponds to the fundamental frequency with a signal-to-noise ratio of high than 70 dB. It is clear that the repetition rate of the pulse train is $\sim$9.44 MHz, corresponding to the cavity round-trip time. As a result, the average output power is about 1.1 mW, corresponding to the pulse energy of about 116.4 pJ.

When pump power is high, mode locking shifts to short wavelength. In this case, different polarization will lead to the switchable wavelength operating in another two center wavelengths (such as the switchable wavelength between 1033.7 and 1029.7 nm or 1029.7 and 1025.7 nm).

On the other hand, we fix the polarization orientation in the case of mode locking at 1033 nm. The spectral width becomes large with the increase of pump power. Fig. 5(a) shows the spectral profiles when the pump powers increase from 54 mW to 70 mW. The inset of the figure shows the spectra on a linear scale. The spectral widths increase from 1.36 nm to 2.11 nm. The pulse durations decrease from 304 ps to 237 ps, as shown in Fig 5(c). For the case of mode locking at 1037 nm, the

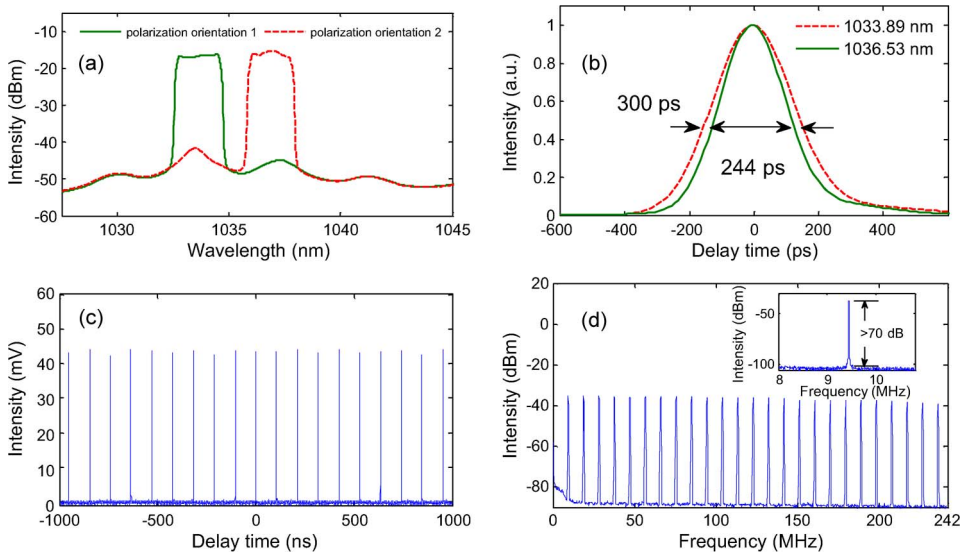

Fig. 4. Switchable wavelength state of the proposed fiber laser in different polarization orientations, (a) the spectra at 1034 nm and 1037 nm, respectively, (b) corresponding pulse width, (c) mode locking pulse train at 1036.89 nm, and (d) corresponding RF spectrum with the inset of the fundamental frequency signal.

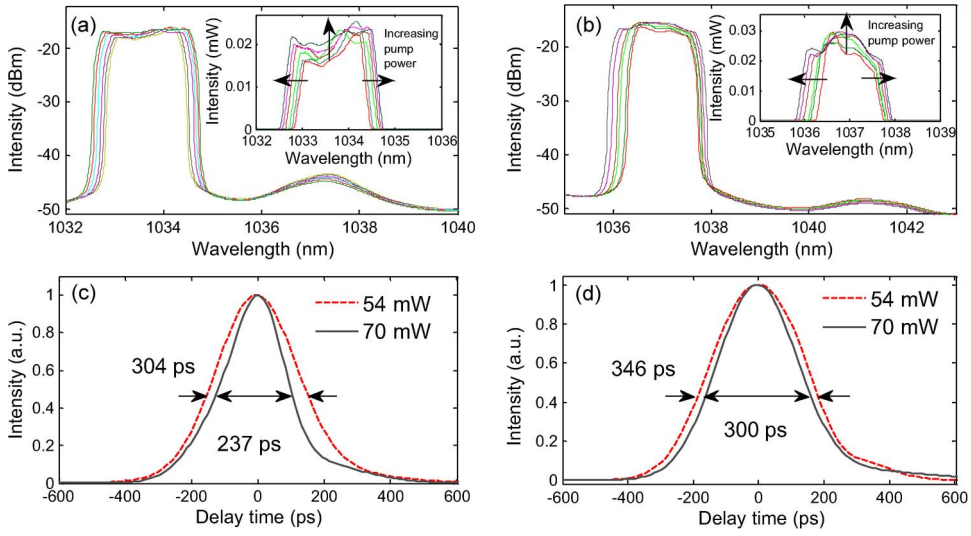

Fig. 5. Evolution of spectra with the increase of the pump powers from 54 mW to 70 mW at 1033 nm band and 1037 nm band, respectively. (a) The evolution of spectra on a log scale. (Inset) Profiles on a linear scale at 1033-nm band. (c) The corresponding waveforms for pump powers of 54 and 70 mW. (b) The evolution of spectra at 1037-nm band. (d) Corresponding waveforms under the pump power of 54 mW and 70 mW.

spectral width can also becomes large with the increase of the pump power, as shown in Fig. 5(b). The spectral widths vary from 1.14 nm to 1.82 nm, and the corresponding pulse widths change from 346 ps to 300 ps, as shown in Fig. 5(d). In general, the average chirps in the long wavelength are larger than the one in the short wavelength. The intensity in the center wavelength is lower than both sides for the 1033-nm band, while it is higher than both sides for the 1037-nm band. We attribute it to the fact that different effective filtering bandwidths result in different mode-locked states. In addition, the center wavelength shifts slightly toward the short wavelength side when the

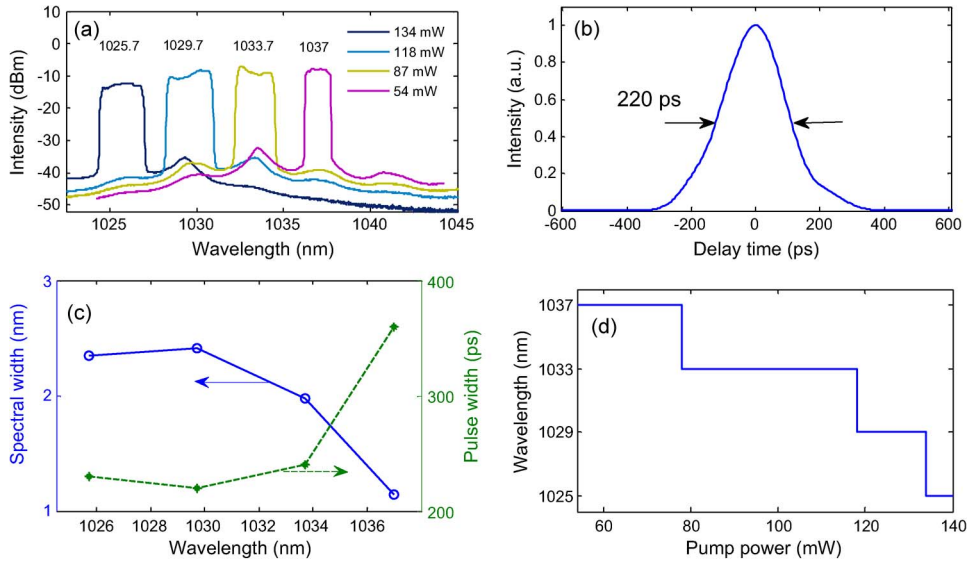

Fig. 6. Mode-locking for different pump powers. (a) The tuning range covers from 1025 nm to 1037 nm, (b) measured pulse profile corresponds to mode-locked spectra at 1029.7 nm, (c) the spectral bandwidth and the pulse duration at different center wavelength, and (d) wavelength regimes of mode locking versus pump power.

pump power increases. The spectral width in the short wavelength is larger than the one in the long wavelength regimes in our experiment. The saturable absorber may play an important role. The SWCNT wall papers in different wavelengths have different saturable-absorption characteristics. Therefore, the pulse width in longer wavelength is larger than the one in short wavelength in our experiment.

As indicated by our experimental results, the tunable wavelength mode-locked fiber laser can be simply realized by increasing the pump powers. As we fix the polarization orientation to the case of 1037-nm band and increase the pump power, CW emission at 1037 nm is observed first, and then, mode locking is achieved when the pump power increases. With the further increase of the pump power and, thus, the variation of the gain and loss distributions, CW emission at short wavelengths become stronger, and then, mode locked states are obtained in the corresponding wavelength region. Fig. 6(a) shows the spectra of mode locking at different pump powers. Self-started stable mode locking states are obtained at 1037, 1034, 1030, and 1026 nm bands corresponding to pump powers of 54, 87, 118, and 134 mW, respectively. In each mode-locked channel, the spectral width becomes large when the pump power increases. The average spacing wavelength of the laser is 3.6 nm and can be slightly changed at different pump power and polarization state. A pulse width of 220 ps corresponding to the widest spectra with a center wavelength of 1029.7 nm is obtained, as shown in Fig. 6(b). The spectral bandwidth and the pulse duration variations are further shown in Fig. 6(c). The spectral bandwidth varied from 1.14 nm to 2.42 nm, and the corresponding pulse width changed from 220 to 360 ps. The wavelength regimes of the mode locking versus of the pump power are shown in Fig. 6(d). Because of the birefringence of the fiber, the center wavelength can be separated. In each regime, the wavelength also varied slightly with the increase of the pump power. In addition, by controlling the polarization orientation of the cavity, the switchable mode locking can also be realized in the cavity between two wavelengths. When the pump power is further increased, the SWCNT wall paper is likely to be damaged. Typically, when the pump power reaches 140 mW, the wall paper is damaged, and the fiber laser loses mode locking.

The proposed wavelength-tunable mode-locked fiber laser exhibits an excellent stability at room temperature. Mode locking around 1033 nm is measured as shown in Fig. 7. The spectra are repeatedly detected 20 times at an interval of 10 min. No significant wavelength shift or peak power

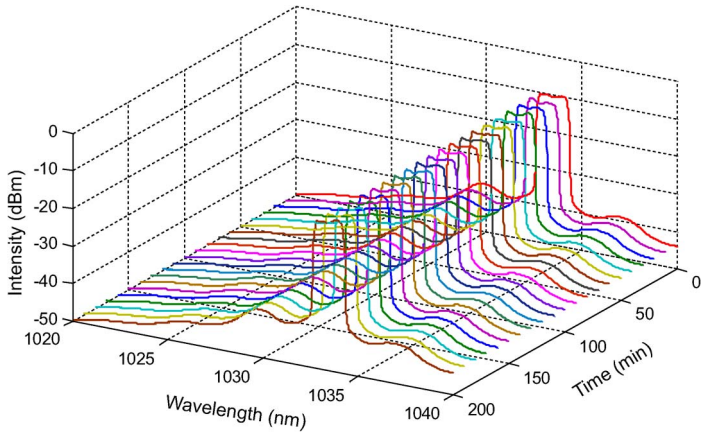

Fig. 7. Stability of the wavelength-tunable mode-locked fiber laser based on SWCNT wall paper.

fluctuation is observed. The mode locking at other wavelength also exhibits similar characteristics, indicating that the proposed fiber laser is stable at room temperature.

The switchable and tunable mode locking can be explained by two mechanisms coexisting in the fiber cavity. First, due to the birefringence of the fiber, changing the bias of the PC can lead to different birefringence of the cavity. Thus different transmission distribution of spectrum can be obtained. When the pump power is above the mode-locked threshold, the switchable mode locking can be obtained. The relationship between the separation of the spectral peaks and the birefringence of the cavity can be expressed as [21]

$$\Delta\lambda = \frac{\lambda^2}{BL} \tag{1}$$

where λ is the center wavelength of the laser, B is the birefringence of the cavity, and L is the length of the cavity. The effective birefringence of the fiber is about 10^{-5}, and therefore, the wavelength separation is calculated as being about 4.9 nm. Considering the fiber is bended into a loop, the actually birefringence is a little higher, and therefore, the wavelength spacing is smaller than the calculated one.

Second, increasing the pump power can lead to the variation of the gain-and-loss distribution, which makes the peak of the spectral modulation shift to other wavelength. When the intensity is above the corresponding threshold, mode locking can be obtained. Thanks to the broadband saturable absorption of the SWCNT wall paper absorber together with the variation of the transmission, the tunable wavelength fiber laser can be achieved.

The intensity-dependent transmission change is due to variation of the inversion condition of YDF. Different pump powers lead to different gain and loss distribution, which ultimately affects the cavity transmission.

Because no additional filter or other wavelength-control components are used in the cavity, the proposed fiber laser automatically operates in the 1030-nm regimes. Furthermore, the SWCNT wall paper has a damage threshold. When the pump power is above the threshold, the proposed fiber laser loses mode locking and cannot be tuned any longer. The characteristics of the wall paper itself also effect the tuning range of the mode locking. Because of these factors in the cavity, the tuning range is limited.

4. Conclusion

A wavelength-switchable and wavelength-tunable mode-locked YDF laser based on the SWCNT wall paper absorber is demonstrated. Benefiting from the broad saturable absorption of the SWCNT wall paper absorber, switchable mode locking is realized by changing the cavity birefringence.

Moreover, the birefringence is enhanced by bending a piece of fiber into a loop. Tunable mode locking is realized by increasing the pump power, which causes the variation of intensity-dependent transmission. The experimental results show that the proposed fiber laser operates stably at room temperature. Furthermore, a wider wavelength tuning range is expected to be obtained by optimizing the fiber cavity in the future.

References

[1] H. Zhang, D. Y. Tang, X. Wu, and L. M. Zhao, "Multi-wavelength dissipative soliton operation of an erbium-doped fiber laser," *Opt. Exp.*, vol. 17, no. 15, pp. 12 692–12 697, Jul. 2009.

[2] H. Zhang, D. Y. Tang, L. M. Zhao, Q. L. Bao, K. P. Loh, B. Lin, and S. C. Tjin, "Compact graphene mode-locked wavelength-tunable erbium-doped fiber lasers: From all anomalous dispersion to all normal dispersion," *Laser Phys. Lett.*, vol. 7, no. 8, pp. 591–596, Aug. 2010.

[3] A. P. Luo, Z. C. Luo, W. C. Xu, V. V. Dvoyrin, V. M. Mashinsky, and E. M. Dianov, "Tunable and switchable dual-wavelength passively mode-locked Bi-doped all-fiber ring laser based on nonlinear polarization rotation," *Laser Phys. Lett.*, vol. 8, no. 8, pp. 601–605, Aug. 2011.

[4] X. H. Li, X. M. Liu, D. Mao, X. H. Hu, and H. Lu, "Tunable and switchable multiwavelength fiber lasers with broadband range based on nonlinear polarization rotation technique," *Opt. Eng.*, vol. 49, no. 9, p. 094303, Sep. 2010.

[5] D. S. Moon, G. Y. Sun, A. X. Lin, X. M. Liu, and Y. J. Chung, "Tunable dual-wavelength fiber laser based on a single fiber Bragg grating in a Sagnac loop interferometer," *Opt. Commun.*, vol. 281, no. 9, pp. 2513–2516, May 2008.

[6] X. J. Zhu, C. H. Wang, S. X. Liu, D. F. Hu, J. J. Wang, and C. Y. Zhu, "Switchable dual-wavelength and passively mode-locked all-normal-dispersion Yb-doped fiber lasers," *IEEE Photon. Tech. Lett.*, vol. 23, no. 14, pp. 956–958, Jul. 2011.

[7] F. Wang, A. G. Rozhin, V. Scardaci, Z. Sun, F. Hennrich, I. H. White, W. I. Milne, and A. C. Ferrari, "Wideband-tuneable, nanotube mode-locked, fibre laser," *Nature Nanotech.*, vol. 3, no. 12, pp. 738–742, Dec. 2008.

[8] X. H. Li, Y. S. Wang, W. Zhao, W. Zhang, Z. Yang, X. H. Hu, H. S. Wang, X. L. Wang, Y. N. Zhang, Y. K. Gong, C. Li, and D. Y. Shen, "All-normal dispersion, figure-eight, tunable passively mode-locked fiber laser with an invisible and changeable intracavity bandpass filter," *Laser Phys.*, vol. 21, no. 5, pp. 940–944, May 2011.

[9] H. Zhang, D. Y. Tang, L. M. Zhao, and N. Xiang, "Coherent energy exchange between components of a vector soliton in fiber lasers," *Opt. Exp.*, vol. 16, no. 17, pp. 12 618–12 623, Aug. 2008.

[10] Z. C. Luo, A. P. Luo, W. C. Xu, H. S. Yin, J. R. Liu, Q. Ye, and Z. J. Fang, "Tunable multiwavelength passively mode-locked fiber ring laser using intracavity birefringence-induced comb filter," *IEEE Photon. J.*, vol. 2, no. 4, pp. 571–577, Aug. 2010.

[11] J. Yao, J. P. Yao, Y. Wang, S. Chuan Tjin, Y. Zhou, Y. L. Lam, J. Liu, and C. Lu, "Active mode locking of tunable multi-wavelength fiber ring laser," *Opt. Commun.*, vol. 191, no. 3–6, pp. 341–345, May 2001.

[12] Z. C. Luo, A. P. Luo, and W. C. Xu, "Stable multiwavelength erbium-doped fibre laser using intensity-dependent loss mechanism with short cavity length," *Electron. Lett.*, vol. 47, no. 20, pp. 1145–1146, Sep. 2011.

[13] X. Zhao, Z. Zheng, L. Liu, Y. Liu, Y. X. Jiang, X. Yang, and J. S. Zhu, "Switchable, dual-wavelength passively mode-locked ultrafast fiber laser based on a single-wall carbon nanotube modelocker and intracavity loss tuning," *Opt. Exp.*, vol. 19, no. 2, pp. 1168–1173, Jan. 2011.

[14] Z. Sun, A. G. Rozhin, F. Wang, V. Scardaci, W. I. Milne, I. H. White, F. Hennrich, and A. C. Ferrari, "L-band ultrafast fiber laser mode locked by carbon nanotubes," *Appl. Phys. Lett.*, vol. 93, no. 6, p. 061114, Aug. 2008.

[15] H. Zhang, D. Y. Tang, R. J. Knize, L. M. Zhao, Q. L. Bao, and K. P. Loh, "Graphene mode locked, wavelength-tunable, dissipative soliton fiber laser," *Appl. Phys. Lett.*, vol. 96, no. 11, p. 111112, Mar. 2010.

[16] S. M. Kobtsev, S. V. Kukarin, and Y. S. Fedotov, "Mode-locked Yb fiber laser with saturable absorber based on carbon nanotubes," *Laser Phys.*, vol. 21, no. 2, pp. 283–286, Feb. 2011.

[17] Z. C. Luo, A. P. Luo, and W. C. Xu, "Tunable and switchable multiwavelength passively mode-locked fiber laser based on SESAM and in-line birefringence comb filter," *IEEE Photon. J.*, vol. 3, no. 1, pp. 64–70, Feb. 2011.

[18] Y. G. Wang, H. R. Chen, X. M. Wen, W. F. Hsieh, and J. Tang, "High efficient sandwich-structured wall paper graphene oxide absorber for Q-switched Nd:GdVO4 laser," *Nano Technol.*, vol. 22, no. 45, p. 455203, Nov. 2011.

[19] N. Akhmediev, J. M. Soto-Crespo, and Ph. Grelu, "Roadmap to ultra-short record high-energy pulses out of laser oscillators," *Phys. Lett. A*, vol. 372, no. 17, pp. 3124–3128, Apr. 2008.

[20] H. Zhang, D. Y. Tang, L. M. Zhao, X. Wu, and H. Y. Tam, "Dissipative vector solitons in a dispersion managed cavity fiber laser with net positive cavity dispersion," *Opt. Exp.*, vol. 17, no. 2, pp. 455–460, Jan. 2009.

[21] G. P. Agrawal, *Nonlinear Fiber Optics*, 4th ed. New York: Academic, 2007.